

CF-ROUTER: CLOSED-FORM SOLUTION FOR EXPERT SELECTION IN MULTIMODAL AGENT LIFELONG LEARNING

006 **Anonymous authors**

007 Paper under double-blind review

ABSTRACT

Multimodal Large Language Models (MLLMs) are increasingly pivotal as lifelong learning agents, tasked with adapting to evolving environments without succumbing to catastrophic forgetting. Current strategies often leverage Mixture-of-Experts (MoE) architectures combined with Low-Rank Adaptation (LoRA) to compartmentalize domain-specific knowledge. However, prevailing routing mechanisms—whether relying on MLLM prompting or heuristic similarity metrics—frequently suffer from low training efficiency or poor alignment within complex multimodal feature spaces. To address these limitations, we introduce **CF-Router**, a novel routing framework grounded in a **closed-form solution**. By leveraging the average-pooled hidden states from the MLLM’s final layer as representative semantic descriptors, we employ a regularized least-squares classifier to precisely identify the optimal expert LoRA. This methodology facilitates analytic, mathematically optimal updates, guaranteeing rapid task identification and seamless adaptation for lifelong learning agents.

1 INTRODUCTION

The pursuit of autonomous agents capable of *lifelong learning* remains a cornerstone objective in artificial intelligence (De Lange & Tuytelaars, 2021; He et al., 2023; Cossu et al., 2024). These agents are required to continuously acquire novel skills and adapt to dynamic domains without erasing previously established knowledge, a challenge known as catastrophic forgetting (McCloskey & Cohen, 1989; Ratcliff, 1990). Multimodal Large Language Models (MLLMs), with their robust generalized reasoning, serve as ideal backbones for such systems (Bai et al., 2025; Li et al., 2024; Chen et al., 2024b). However, conventional sequential fine-tuning of MLLMs typically results in significant performance erosion on earlier tasks (Guo et al., 2025a; Chen et al., 2025).

To counteract this, parameter-efficient continual learning frameworks, notably those integrating MoE with LoRA, have shown promise. A prominent example, Zhao et al. (2025), dedicates distinct LoRA experts to specific domains. The efficacy of this architecture hinges on the **router**, which is responsible for selecting the appropriate expert for a given input. Nevertheless, existing routers face substantial drawbacks: similarity-based approaches (e.g., utilizing cosine similarity of prototypes) often struggle with the non-linear boundaries of multimodal distributions (Chen et al., 2024a; Huai et al., 2025), while MLLM-based routers, which rely on the model for self-selection, introduce high training overhead and potential privacy concerns if replay-based methods are used (Zhao et al., 2025), rendering them impractical for real-time applications.

In this work, we present a scalable and efficient solution: the **Closed-Form Router (CF-Router)**. Our approach is distinguished by two key attributes: it is **analytic** and **replay-free**. The analytic nature ensures that router updates are derived via closed-form solution rather than stochastic gradient descent (SGD), thereby avoiding interference with weights from prior tasks and eliminating a primary source of catastrophic forgetting (Wang et al., 2024). The replay-free design addresses the storage and privacy constraints inherent to MLLMs (Zhao et al., 2025). Storing high-resolution images or lengthy text instructions demands excessive storage, which is unsuitable for edge or large-scale deployments. Furthermore, given that MLLMs are trained on trillion-scale datasets, replaying a limited subset of samples is often insufficient to preserve the model’s vast knowledge base and risks overfitting.

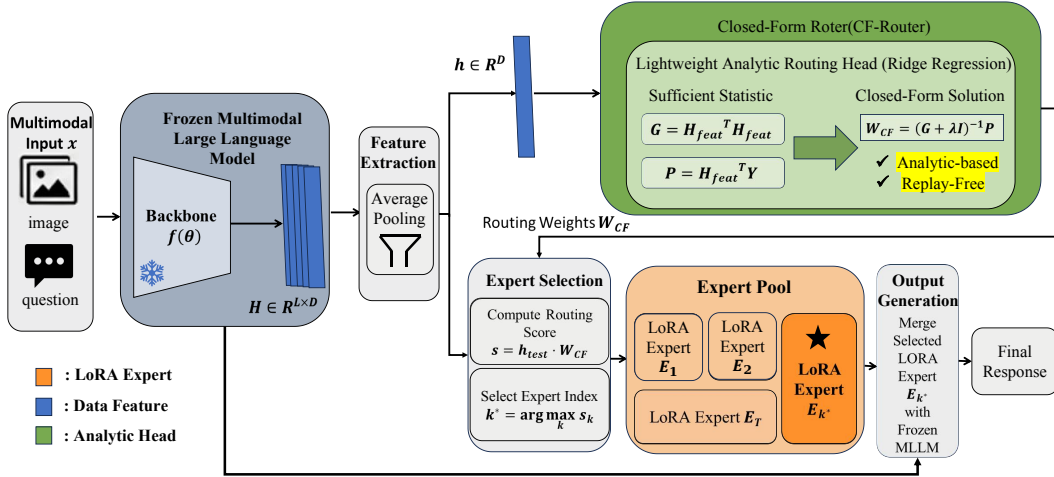


Figure 1: Overview of the proposed method

Technically, our method extracts rich semantic representations from the frozen MLLM’s final layer, applies average pooling to condense the sequence, and maps these features to expert indices via an analytically solved linear head.

Our contributions are as follows:

- We identify the bottleneck in existing MLLM continual learning routers and propose the integration of a closed-form solution to decouple expert selection from gradient-based optimization.
- We introduce the CF-Router architecture, which utilizes the MLLM’s last-layer hidden states to solve the routing problem analytically, ensuring rapid adaptation with zero backpropagation costs for the router.
- We frame this contribution within the context of Agent Lifelong Learning, enabling agents to instantly index and retrieve domain-specific skills.

2 METHODOLOGY

An overview of our proposed framework is illustrated in Figure 1. Our goal is to enable an MLLM agent to learn a sequence of tasks $\mathcal{T} = \{1, \dots, T\}$ sequentially. We adopt an architecture where a shared frozen MLLM backbone f_θ is augmented with a pool of trainable LoRA experts $\mathcal{E} = \{E_1, \dots, E_T\}$, where each expert E_t specializes in a specific task or domain. The core innovation of our work is the mechanism for selecting the appropriate expert E_k for a test instance x using a closed-form solution.

2.1 PRELIMINARIES: MLLM-CL

The MLLM-CL framework prevents forgetting by isolating parameters, assigning a specific LoRA module to each task. During inference, a router must predict the task identity k to activate the correct expert. We propose to solve this task identity prediction using a regularized least-squares (Ridge Regression) approach applied directly to the MLLM’s hidden features.

2.2 THE CF-ROUTER ARCHITECTURE

The proposed CF-Router operates in two distinct stages: Feature Extraction and Closed-Form Decision.

108 2.2.1 FEATURE EXTRACTION VIA HIDDEN STATES
109

110 Given a multimodal input x (comprising image embeddings and text instructions), the frozen MLLM
111 backbone processes the sequence. Let $H \in \mathbb{R}^{L \times D}$ denote the hidden states of the last transformer
112 layer of the MLLM, where L is the sequence length and D is the hidden dimension. To obtain a
113 fixed-size representation suitable for the analytic solver, we apply average pooling across the sequence
114 dimension:

$$115 \quad h = \frac{1}{L} \sum_{i=1}^L H_i \quad (1)$$

117 where $h \in \mathbb{R}^D$ serves as the robust semantic signature of the current input context. In our implementa-
118 tion, $D = 4096$, corresponding to the hidden dimension of the MLLM’s last layer.

120 2.2.2 CLOSED-FORM EXPERT SELECTION
121

122 The router’s objective is to map the semantic feature h extracted from the backbone directly to an
123 expert index $y \in \{1, \dots, T\}$. We treat this as a regression problem where the target is the one-hot
124 encoding of the expert index. The optimal weights $W_{CF} \in \mathbb{R}^{D \times T}$ for the routing head are computed
125 by minimizing the regularized mean squared error:

$$126 \quad W_{CF} = \arg \min_W \|H_{feat}W - Y\|_F^2 + \lambda \|W\|_F^2 \quad (2)$$

127 where H_{feat} is the matrix of collected hidden features from observed tasks, Y is the matrix of expert
128 labels, and λ is a regularization parameter. Following McDonnell et al. (2023), the solution is given
129 by the closed-form equation:

$$130 \quad W_{CF} = (H_{feat}^T H_{feat} + \lambda I)^{-1} H_{feat}^T Y \quad (3)$$

131 In a lifelong learning scenario, we do not need to store all raw data H_{feat} . Instead, we incrementally
132 update the Gram matrix $G = H_{feat}^T H_{feat}$ and the correlation matrix $P = H_{feat}^T Y$. When a new
133 task T arrives, we update G and P using the new task data and recompute W_{CF} via matrix inversion.
134 This process is computationally efficient and requires no gradient descent.

135 2.3 INFERENCE AND ROUTING
136

137 During inference, for an incoming query x_{test} , we extract its pooled feature h_{test} . The router
138 computes the relevance scores s for all available experts:

$$140 \quad s = h_{test} W_{CF} \quad (4)$$

141 The system selects the expert corresponding to the maximum score:

$$142 \quad k^* = \arg \max_k s_k \quad (5)$$

143 The corresponding LoRA module E_{k^*} is then merged with the backbone to generate the final response.
144 This ensures that the agent leverages the precise domain knowledge required for the current interaction
145 without interference from other domains. To enhance computational efficiency during inference, we
146 adopt a cache-based optimization strategy inspired by the design of MLLM-CL (Zhao et al., 2025): a
147 single forward pass is executed through the backbone network (vision encoder and language model)
148 to cache the hidden states of each layer (including KV Cache). Subsequent lightweight components,
149 such as the CF-Router and task-specific experts, directly reuse these cached states, thereby avoiding
150 redundant computations.

151 We present the training and inference procedures for our Continual Learning framework with the
152 Closed-Form Router (CF-Router). The training process decouples the optimization of domain-specific
153 experts (via Gradient Descent) from the router updates (via Analytic Solution), ensuring efficiency
154 and stability.

155 3 EXPERIMENT
156157 3.1 EXPERIMENTAL SETUP AND DATASETS
158

159 To evaluate the effectiveness of CF-Router in multimodal lifelong learning, we adopt the Domain
160 Continual Learning (DCL) benchmark proposed in MLLM-CL (Zhao et al., 2025). The benchmark
161 consists of five diverse and challenging domains:

162 **Algorithm 1** Lifelong Learning with CF-Router (Training Phase)

163
Require: Sequence of tasks $\mathcal{T} = \{1, \dots, T\}$
Require: Frozen MLLM backbone f_θ
Require: Regularization λ , Buffer for G, P

164 1: **for** each task $t \in \mathcal{T}$ with dataset \mathcal{D}_t **do**
165 2: **Initialize** new LoRA expert E_t
166 3: {Phase 1: Accumulate Statistics for Router (Closed-Form)}
167 4: **for** each batch (x, y) in \mathcal{D}_t **do**
168 5: Extract last-layer hidden states: $H = f_\theta(x)$
169 6: Average Pooling: $h = \text{AvgPool}(H)$
170 7: Construct one-hot target y_{router} for task t
171 8: Update Gram matrix: $G \leftarrow G + h^T h$
172 9: Update Correlation matrix: $P \leftarrow P + h^T y_{\text{router}}$
173 10: **end for**
174 11: {Phase 2: Train Expert (Gradient Descent)}
175 12: **for** each batch (x, y) in \mathcal{D}_t **do**
176 13: Forward pass with Expert E_t : $\hat{y} = f_{\theta, E_t}(x)$
177 14: Compute LLM Loss: $\mathcal{L} = \text{CrossEntropy}(\hat{y}, y)$
178 15: Update E_t via backpropagation (keep f_θ frozen)
179 16: **end for**
180 17: {Phase 3: Update Router Weights Analytically}
181 18: $W_{CF} = (G + \lambda I)^{-1} P$
182 19: Store/Freeze Expert E_t
183 20: **end for**

185
Algorithm 2 Inference with CF-Router

186
Require: Test instance x_{test}
187
Require: Frozen MLLM f_θ , Router W_{CF}
188
Require: Pool of Experts $\mathcal{E} = \{E_1, \dots, E_T\}$

189 1: {Step 1: Router Decision}
190 2: Extract last-layer hidden states: $H = f_\theta(x_{\text{test}})$
191 3: Average Pooling: $h = \text{AvgPool}(H)$
192 4: Calculate Scores: $s = h W_{CF}$
193 5: Select Expert Index: $k^* = \arg \max_k s_k$
194 6: {Step 2: Generation}
195 7: Activate LoRA Expert E_{k^*}
196 8: Generate Response: $y_{\text{pred}} = f_{\theta, E_{k^*}}(x_{\text{test}})$
197 9: **return** y_{pred}

200 1. **Remote Sensing (RS):** Focused on satellite imagery understanding and spatial reasoning.
201 2. **Medical (Med):** Comprising clinical images and pathology slides for diagnostic question answering.
202 3. **Autonomous Driving (AD):** Involving ego-centric view analysis and traffic scene understanding.
203 4. **Science (Sci):** Covering multi-disciplinary scientific diagrams and textbook problems.
204 5. **Finance (Fin):** Including chart parsing and financial report interpretation tasks.

205 For each domain, the agent learns a specific task sequentially. We utilize **LLaVA-1.5-7B** (Liu et al., 2024) and **InternVL-Chat-V1.0** (Chen et al., 2024b) as our base MLLM architectures. CF-Router adopts the same expert descriptions and task definitions as the MLLM-based router in MLLM-CL (Zhao et al., 2025). The detailed prompt template for expert selection is provided in Figure 2.

206
207
208 3.2 IMPLEMENTATION DETAILS AND HYPERPARAMETERS

209
210 Our framework is implemented using PyTorch. In the CF-Router, we directly use the average-pooled
211 hidden states of the MLLM’s last layer (dimension $D = 4096$) as the input to the closed-form solver,

216
 217 You are a helpful assistant router. There are five expert models,
 218 each specializing in one of the following domains: finance (stock),
 219 science, medical imaging, autonomous driving, and remote sensing.
 220
 221 Your task is to select the most suitable model based on the provided
 222 visual content, user question, and model descriptions. Consider the
 223 expertise of each model carefully and select the one best equipped
 224 to handle the given question.
 225
Important Instructions:
 226 • Respond **only** with the letter (A, B, C, D, E) corresponding to the
 227 most suitable model.
 228 • Do not attempt to answer the user's question directly.
Model Pool:
 229 • **A:** A financial expert specializing in stock market analysis using
 230 candlestick charts. This model excels at trend prediction and
 231 technical indicator analysis.
 232 • **B:** A science expert with proficiency in biology, map
 233 interpretation, physics, and chemistry.
 234 • **C:** A medical imaging expert, primarily focused on pathology,
 235 including cell sections and natural images of medical conditions.
 236 • **D:** An autonomous driving expert specializing in ego-view scene
 237 understanding, including coordinate prediction and action
 238 planning and other driving-related tasks. The input image is
 239 an image concatenated by 6 camera views.
 240 • **E:** A remote sensing expert, adept at analyzing aerial or
 241 satellite images. This model excels at object counting, presence
 242 detection, and area estimation.
 243 Here is the user's question: [User's Question]

Figure 2: Prompt of the router selector.

244
 245 without any additional projection. The ridge regression regularization coefficient is set to $\lambda = 0.1$.
 246 For the Expert LoRAs, we use a rank of $r = 128$ and a scaling factor of $\alpha = 256$, following the
 247 standard configuration in (Zhao et al., 2025). Training is conducted using the AdamW optimizer with
 248 a learning rate of 2×10^{-5} and a batch size of 128.
 249

250 3.3 EVALUATION METRICS

251 To quantify the performance of multimodal lifelong learning, we report four key metrics. Let $a_{i,j}$
 252 denote the performance (e.g., accuracy) on task j after the agent has finished learning task i , and T
 253 be the total number of tasks.

- 254 • **MAA** (Mean Average Accuracy): The average performance across all tasks observed so far at each
 255 curriculum stage:
 256

$$\text{MAA} = \frac{1}{T} \sum_{i=1}^T \left(\frac{1}{i} \sum_{j=1}^i a_{i,j} \right) \quad (6)$$

- 257 • **MFT** (Mean Final Task): The average performance across all tasks after the entire sequence of T
 258 tasks has been learned:
 259

$$\text{MFT} = \frac{1}{T} \sum_{j=1}^T a_{T,j} \quad (7)$$

- 260 • **MFN** (Mean Final New): The average performance on each task immediately after it is learned:
 261

$$\text{MFN} = \frac{1}{T} \sum_{i=1}^T a_{i,i} \quad (8)$$

270
271 Table 1: Results for LLaVA-1.5-based domain continual learning in MLLM-CL benchmark. Baseline
272 results are quoted from (Zhao et al., 2025). * denotes the original method with replay data.

Method	Task Performance					Aggregate Metrics			
	RS	Med	AD	Sci	Fin	MFT↑	MFN↑	MAA↑	BWT↑
Zeroshot	32.29	28.28	15.59	35.55	62.56	34.85	-	-	-
Oracle	81.06	65.83	54.17	56.86	91.14	69.81	-	-	-
LoRA-FT (Hu et al., 2021)	69.65	41.59	25.43	40.88	87.45	64.98	53.00	61.13	-14.97
LoRA-FT* (Hu et al., 2021)	76.54	50.27	43.01	43.32	89.85	66.32	60.60	64.72	-7.15
O-LoRA (Wang et al., 2023)	74.64	44.42	30.02	41.47	87.15	65.16	55.54	62.12	-12.03
O-LoRA* (Wang et al., 2023)	76.94	41.17	34.18	39.61	83.22	60.49	55.02	60.73	-6.83
MoELoRA (Chen et al., 2024a)	77.54	41.85	27.62	40.13	86.75	64.94	54.78	61.76	-12.70
MoELoRA* (Chen et al., 2024a)	77.63	49.54	39.08	41.04	89.21	66.24	59.30	64.81	-8.68
CL-MoE (Huai et al., 2025)	71.34	46.84	26.33	41.17	88.74	66.06	54.88	61.79	-13.96
CL-MoE* (Huai et al., 2025)	76.58	52.31	39.65	45.64	90.21	66.65	60.88	64.95	-7.22
HiDe (Guo et al., 2025a)	74.31	48.95	33.21	38.54	81.55	60.77	55.31	60.68	-6.82
HiDe* (Guo et al., 2025a)	74.80	42.29	34.03	38.01	79.22	60.83	53.67	61.81	-8.95
SEFE (Chen et al., 2025)	77.26	50.37	37.21	40.87	86.82	65.01	58.51	63.63	-8.13
SEFE* (Chen et al., 2025)	78.43	52.85	46.21	47.76	89.33	66.89	62.92	66.51	-4.97
DISCO (Guo et al., 2025b)	76.03	45.20	43.79	42.33	88.95	64.43	59.26	63.35	-6.46
DISCO* (Guo et al., 2025b)	77.78	46.25	50.45	49.51	89.71	65.27	62.74	64.92	-3.17
Ours	81.28	65.61	54.68	56.89	91.14	69.92	69.92	71.29	0.00

290
291 Table 2: Results for InternVL-Chat-V1.0-based domain continual learning in MLLM-CL benchmark.
292 Baseline results are quoted from (Zhao et al., 2025). * denotes the original method with replay data.

Method	Task Performance					Aggregate Metrics			
	RS	Med	AD	Sci	Fin	MFT↑	MFN↑	MAA↑	BWT↑
Zeroshot	31.16	29.81	14.06	33.93	64.32	34.66	-	-	-
Oracle	81.49	66.42	54.56	54.48	91.24	69.64	-	-	-
LoRA-FT (Hu et al., 2021)	69.93	52.17	33.04	42.67	91.07	69.06	57.78	65.22	-14.11
LoRA-FT* (Hu et al., 2021)	77.06	47.55	42.67	43.31	91.44	69.43	60.41	67.45	-11.28
MoELoRA (Chen et al., 2024a)	69.90	52.08	33.17	42.19	90.58	68.83	57.58	65.97	-14.06
MoELoRA* (Chen et al., 2024a)	76.74	52.65	38.81	42.15	89.84	67.90	60.04	66.01	-9.83
HiDe (Guo et al., 2025a)	75.40	57.66	36.73	41.48	88.59	65.26	59.97	65.94	-6.60
HiDe* (Guo et al., 2025a)	53.17	52.61	40.85	47.04	89.17	64.20	56.57	61.06	-9.54
DISCO (Guo et al., 2025b)	75.12	50.69	52.41	50.67	90.86	68.85	63.95	68.14	-6.12
DISCO* (Guo et al., 2025b)	77.90	47.50	49.13	49.37	90.92	68.55	62.96	67.81	-6.98
Ours	81.52	64.42	54.62	53.12	91.10	68.96	68.96	70.74	0.00

- **BWT** (Backward Transfer): The average change in performance on previously learned tasks after acquiring new knowledge. A BWT of 0 indicates zero forgetting:

$$\text{BWT} = \frac{1}{T-1} \sum_{j=1}^{T-1} (a_{T,j} - a_{j,j}) \quad (9)$$

3.4 MAIN RESULTS AND COMPARATIVE ANALYSIS

Table 1 and Table 2 present the performance of CF-Router compared to various state-of-the-art continual learning methods on the LLaVA-1.5 and InternVL backbones, respectively. Several observations can be made:

Superior Overall Performance: Our method consistently outperforms all baselines across every domain and metric. For example, on LLaVA-1.5, we achieve an MAA of 71.29%, which is significantly higher than the best baseline DISCO* (64.92%). In several domains like Remote Sensing (RS) and Science (Sci), our performance matches the Oracle (sequential fine-tuning on each task individually with full access to data), demonstrating the efficacy of our expert isolation and precise routing.

Zero Forgetting (BWT=0): A standout result is the BWT of 0.00 across all experiments. While baseline methods like MoELoRA and SEFE suffer from negative backward transfer (ranging from

-14.97 to -3.17), CF-Router completely eliminates catastrophic forgetting. This is because our architecture stores domain-specific knowledge in isolated LoRA experts, and our closed-form router ensures that the correct expert is indexed without interference from subsequent tasks.

Independence from Replay Data: Most high-performing baselines (marked with *) rely on replayed data from previous tasks to maintain performance. In contrast, CF-Router achieves superior results without any data replay, making it more privacy-preserving and storage-efficient for real-world agentic deployments.

3.5 ROUTING ANALYSIS AND ORDER INVARIANCE

The core strength of CF-Router lies in its ability to accurately identify task identities in an analytic-based manner. As shown in Table 3 and Table 4, the routing accuracy remains near 100% across all domains. This high precision is attributed to the rich semantic features present in the MLLM’s hidden states, which provide sufficient discriminative power to distinguish between task domains in the multimodal feature space.

Mathematical Order Invariance: A unique property of our closed-form solution is its robustness to task sequence. Traditional gradient-based routers (e.g., in MoELoRA) are sensitive to the order of tasks due to the sequential nature of backpropagation. In contrast, our router’s weights W_{CF} are derived from the matrices G and P , which are updated via simple summation (Algorithm 1). Since summation is commutative, the final W_{CF} is mathematically identical regardless of the order in which task statistics are accumulated. Our experiments over 120 task permutations confirm this, with a standard deviation of 0.000 for all metrics.

3.6 COMPUTATIONAL EFFICIENCY ANALYSIS

The CF-Router provides significant computational advantages over gradient-based or prompt-based routing mechanisms. We analyze its efficiency in terms of time and space complexity.

Time Complexity: The computational cost is divided into the incremental update phase and the inference phase.

- Update Phase:** For a task with N_t samples, the time complexity for accumulating the matrices G and P is $O(N_t \cdot D^2)$, where D is the hidden dimension. The analytic solution for W_{CF} involves a matrix inversion and a matrix multiplication, resulting in a complexity of $O(D^3 + D^2 \cdot T)$, where T is the number of experts. Since D is fixed and $T \ll D$, the update is near-instantaneous.
- Inference Phase:** For a single test instance, the routing score calculation $s = hW_{CF}$ has a time complexity of $O(D \cdot T)$. This is negligible compared to the $O(L \cdot D_{model}^2)$ complexity of the MLLM forward pass (where L is sequence length), ensuring minimal added latency.

Space Complexity: CF-Router is highly memory-efficient as it does not require storing raw features H_{feat} or replaying data.

- Training Storage:** To support lifelong learning, we only maintain the matrices $G \in \mathbb{R}^{D \times D}$ and $P \in \mathbb{R}^{D \times T}$. The total space complexity is $O(D^2 + D \cdot T)$. For $D = 4096$, the Gram matrix G occupies only 64 MB (in float32), which is constant regardless of the number of training samples.
- Model Weights:** The router head $W_{CF} \in \mathbb{R}^{D \times T}$ introduces only $D \cdot T$ additional parameters, which is infinitesimal compared to the billions of parameters in the MLLM backbone.

4 RELATED WORK

Traditional continual learning (CL) mitigates catastrophic forgetting through mechanisms such as regularization (Kirkpatrick et al., 2017; Li & Hoiem, 2017), replay (Lavda et al., 2018; Buzzega et al., 2020), or parameter isolation (Rusu et al., 2016; Mallya & Lazebnik, 2018). However, in the context of Large Language Models (LLMs), these methods face significant bottlenecks due to high computational overhead or risks of privacy leakage. This has prompted a shift toward Parameter-Efficient Fine-Tuning (PEFT) paradigms Hu et al. (2021). For instance, O-LoRA (Wang

378 Table 3: CF-Router performance on LLaVA-1.5-7B at the last lifelong learning stage. Results are
 379 reported as mean \pm standard deviation across 120 task permutations.

381	Domain	Router Acc	Expert Acc
382	RS	1.0000 \pm .0000	0.8128 \pm .0000
383	Med	1.0000 \pm .0000	0.6561 \pm .0000
384	AD	1.0000 \pm .0000	0.5468 \pm .0000
385	Sci	0.9993 \pm .0000	0.5689 \pm .0000
386	Fin	1.0000 \pm .0000	0.9114 \pm .0000
387	AVERAGE	0.9999 \pm .0000	0.6992 \pm .0000

389 Table 4: CF-Router performance on InternVL-Chat-V1.0 (ViT-6B-Vicuna-7B) at the last lifelong
 390 learning stage. Results are reported as mean \pm standard deviation across 120 task permutations.

392	Domain	Router Acc	Expert Acc
393	RS	1.0000 \pm .0000	0.8152 \pm .0000
394	Med	1.0000 \pm .0000	0.6442 \pm .0000
395	AD	1.0000 \pm .0000	0.5462 \pm .0000
396	Sci	0.9999 \pm .0000	0.5312 \pm .0000
397	Fin	1.0000 \pm .0000	0.9110 \pm .0000
398	AVERAGE	1.0000 \pm .0000	0.6896 \pm .0000

401 et al., 2023) effectively reduces inter-task interference under replay-free conditions by employing
 402 orthogonal subspace constraints. Extending these concepts to Multimodal Large Language Models
 403 (MLLMs), the CoIN benchmark (Chen et al., 2024a) reveals that forgetting in MLLMs primarily
 404 stems from a failure in instruction alignment rather than a loss of intrinsic knowledge. Inspired by
 405 this finding, MoELoRA (Chen et al., 2024a) and CL-MoE (Huai et al., 2025) integrate Mixture-of-
 406 Experts (MoE) architectures, utilizing task-driven gating and dual-momentum routing mechanisms,
 407 respectively, to balance adaptation between new and old tasks while maintaining parameter efficiency.
 408 Furthermore, HiDe (Guo et al., 2025a) proposes a decoupling strategy based on layer-wise sensitivity
 409 differences, featuring bottom-layer specific expansion and top-layer general fusion to enhance
 410 efficiency. Addressing the nature of catastrophic forgetting, SEFE (Chen et al., 2025) distinguishes
 411 between surface-level style forgetting and essential knowledge forgetting, validating the importance of
 412 style diversification for performance maintenance. Additionally, for distributed environments, DISCO
 413 (Guo et al., 2025b) introduces dynamic knowledge organization and selective subspace activation,
 414 effectively resolving data heterogeneity and task conflicts in federated continual instruction tuning.

415 5 CONCLUSION

417 In this paper, we introduced **CF-Router**, a novel routing mechanism designed for efficient and robust
 418 expert selection in multimodal agent lifelong learning. By leveraging the closed-form analytic solution
 419 of ridge regression directly on the MLLM’s last-layer hidden states, we decouple the optimization of
 420 the routing logic from gradient-based training. Our approach achieves near-perfect routing accuracy
 421 across diverse domains such as remote sensing, medical imaging, and autonomous driving, while
 422 ensuring zero catastrophic forgetting ($BWT=0$) without the need for data replay. Furthermore, we
 423 mathematically demonstrated and experimentally verified the order-invariance of our router, providing
 424 a stable and reliable foundation for agents to acquire new skills sequentially. The analytic-based
 425 nature and minimal inference overhead of CF-Router make it highly suitable for real-time, scalable
 426 lifelong learning applications in complex multimodal environments.

428 REFERENCES

430 Shuai Bai, Keqin Chen, Xuejing Liu, Jialin Wang, Wenbin Ge, Sibo Song, Kai Dang, Peng Wang,
 431 Shijie Wang, Jun Tang, Humen Zhong, Yuanzhi Zhu, Mingkun Yang, Zhaohai Li, Jianqiang Wan,
 Pengfei Wang, Wei Ding, Zheren Fu, Yiheng Xu, Jiabo Ye, Xi Zhang, Tianbao Xie, Zesen Cheng,

- 432 Hang Zhang, Zhibo Yang, Haiyang Xu, and Junyang Lin. Qwen2.5-vl technical report. *arXiv*
 433 *preprint arXiv:2502.13923*, 2025.
- 434
- 435 Pietro Buzzega, Matteo Boschini, Angelo Porrello, Davide Abati, and Simone Calderara. Dark
 436 experience for general continual learning: a strong, simple baseline. *Advances in neural information*
 437 *processing systems*, 33:15920–15930, 2020.
- 438 Cheng Chen, Junchen Zhu, Xu Luo, Hengtao Shen, Jingkuan Song, and Lianli Gao. Coin: A
 439 benchmark of continual instruction tuning for multimodel large language models. *Advances in*
 440 *Neural Information Processing Systems*, 37:57817–57840, 2024a.
- 441
- 442 Jinpeng Chen, Runmin Cong, Yuzhi Zhao, Hongzheng Yang, Guangneng Hu, Horace Ip, and Sam
 443 Kwong. Sefc: Superficial and essential forgetting eliminator for multimodal continual instruction
 444 tuning. In *Forty-second International Conference on Machine Learning*, 2025.
- 445 Zhe Chen, Jiannan Wu, Wenhui Wang, Weijie Su, Guo Chen, Sen Xing, Muyan Zhong, Qinglong
 446 Zhang, Xizhou Zhu, Lewei Lu, et al. Internvl: Scaling up vision foundation models and aligning
 447 for generic visual-linguistic tasks. In *Proceedings of the IEEE/CVF Conference on Computer*
 448 *Vision and Pattern Recognition*, pp. 24185–24198, 2024b.
- 449 Andrea Cossu, Antonio Carta, Lucia Passaro, Vincenzo Lomonaco, Tinne Tuytelaars, and Davide
 450 Bacciu. Continual pre-training mitigates forgetting in language and vision. *Neural Networks*, 179:
 451 106492, 2024.
- 452
- 453 Matthias De Lange and Tinne Tuytelaars. Continual prototype evolution: Learning online from non-
 454 stationary data streams. In *Proceedings of the IEEE/CVF international conference on computer*
 455 *vision*, pp. 8250–8259, 2021.
- 456 Haiyang Guo, Fanhu Zeng, Ziwei Xiang, Fei Zhu, Da-Han Wang, Xu-Yao Zhang, and Cheng-Lin Liu.
 457 Hide-llava: Hierarchical decoupling for continual instruction tuning of multimodal large language
 458 model. *arXiv preprint arXiv:2503.12941*, 2025a.
- 459
- 460 Haiyang Guo, Fanhu Zeng, Fei Zhu, Wenzhuo Liu, Da-Han Wang, Jian Xu, Xu-Yao Zhang, and
 461 Cheng-Lin Liu. Federated continual instruction tuning. *arXiv preprint arXiv:2503.12897*, 2025b.
- 462 Jinghan He, Haiyun Guo, Ming Tang, and Jinqiao Wang. Continual instruction tuning for large
 463 multimodal models. *arXiv preprint arXiv:2311.16206*, 2023.
- 464
- 465 Edward J Hu, Yelong Shen, Phillip Wallis, Zeyuan Allen-Zhu, Yuanzhi Li, Shean Wang, Lu Wang,
 466 and Weizhu Chen. Lora: Low-rank adaptation of large language models. *arXiv preprint*
 467 *arXiv:2106.09685*, 2021.
- 468 Tianyu Huai, Jie Zhou, Xingjiao Wu, Qin Chen, Qingchun Bai, Ze Zhou, and Liang He. Cl-moe:
 469 Enhancing multimodal large language model with dual momentum mixture-of-experts for continual
 470 visual question answering. *arXiv preprint arXiv:2503.00413*, 2025.
- 471 James Kirkpatrick, Razvan Pascanu, Neil Rabinowitz, Joel Veness, Guillaume Desjardins, Andrei A
 472 Rusu, Kieran Milan, John Quan, Tiago Ramalho, Agnieszka Grabska-Barwinska, et al. Overcoming
 473 catastrophic forgetting in neural networks. *Proceedings of the national academy of sciences*, 114
 474 (13):3521–3526, 2017.
- 475
- 476 Frantzeska Lavda, Jason Ramapuram, Magda Gregorova, and Alexandros Kalousis. Continual
 477 classification learning using generative models. *arXiv preprint arXiv:1810.10612*, 2018.
- 478 Bo Li, Yuanhan Zhang, Dong Guo, Renrui Zhang, Feng Li, Hao Zhang, Kaichen Zhang, Yanwei
 479 Li, Ziwei Liu, and Chunyuan Li. Llava-onevision: Easy visual task transfer. *arXiv preprint*
 480 *arXiv:2408.03326*, 2024.
- 481
- 482 Zhizhong Li and Derek Hoiem. Learning without forgetting. *IEEE transactions on pattern analysis*
 483 *and machine intelligence*, 40(12):2935–2947, 2017.
- 484
- 485 Haotian Liu, Chunyuan Li, Yuheng Li, and Yong Jae Lee. Improved baselines with visual instruction
 486 tuning. In *Proceedings of the IEEE/CVF Conference on Computer Vision and Pattern Recognition*,
 487 pp. 26296–26306, 2024.

- 486 Arun Mallya and Svetlana Lazebnik. Packnet: Adding multiple tasks to a single network by iterative
 487 pruning. In *Proceedings of the IEEE conference on Computer Vision and Pattern Recognition*, pp.
 488 7765–7773, 2018.
- 489 Michael McCloskey and Neal J Cohen. Catastrophic interference in connectionist networks: The
 490 sequential learning problem. In *Psychology of learning and motivation*, volume 24, pp. 109–165.
 491 Elsevier, 1989.
- 492 Mark D McDonnell, Dong Gong, Amin Parvaneh, Ehsan Abbasnejad, and Anton Van den Hengel.
 493 Ranpac: Random projections and pre-trained models for continual learning. *Advances in Neural
 494 Information Processing Systems*, 36:12022–12053, 2023.
- 495 Roger Ratcliff. Connectionist models of recognition memory: constraints imposed by learning and
 496 forgetting functions. *Psychological review*, 97(2):285, 1990.
- 497 Andrei A Rusu, Neil C Rabinowitz, Guillaume Desjardins, Hubert Soyer, James Kirkpatrick, Koray
 498 Kavukcuoglu, Razvan Pascanu, and Raia Hadsell. Progressive neural networks. *arXiv preprint
 499 arXiv:1606.04671*, 2016.
- 500 Liyuan Wang, Xingxing Zhang, Hang Su, and Jun Zhu. A comprehensive survey of continual learning:
 501 Theory, method and application. *IEEE transactions on pattern analysis and machine intelligence*,
 502 46(8):5362–5383, 2024.
- 503 Xiao Wang, Tianze Chen, Qiming Ge, Han Xia, Rong Bao, Rui Zheng, Qi Zhang, Tao Gui, and
 504 Xuanjing Huang. Orthogonal subspace learning for language model continual learning. *arXiv
 505 preprint arXiv:2310.14152*, 2023.
- 506 Hongbo Zhao, Fei Zhu, Haiyang Guo, Meng Wang, Rundong Wang, Gaofeng Meng, and Zhaoxiang
 507 Zhang. Mllm-cl: Continual learning for multimodal large language models. *arXiv preprint
 508 arXiv:2506.05453*, 2025.
- 509
 510
 511
 512
 513
 514
 515
 516
 517
 518
 519
 520
 521
 522
 523
 524
 525
 526
 527
 528
 529
 530
 531
 532
 533
 534
 535
 536
 537
 538
 539